P5.19 ANOTHER METHOD FOR GROUND TARGET IDENTIFICATION AND FILTERING USING SPECTRAL PROCESSING OF DUAL-POLARIZATION RETURNS

Frédéric Fabry* and Jonathan Gadoury
McGill University, Montreal, Quebec, Canada

1. WHY ANOTHER GROUND TARGET ID METHOD

Ground targets present a particular challenge at the McGill Radar Observatory. First, we have quite a lot of them, not only because of our towering view over a sedimental plain and a large city, but also because of the sidelobes from our 1960s vintage 9-m antenna. To complicate matters, we scan rapidly (6 RPM), and our radar system has a fair bit of phase noise. The net result is that ground targets have an unusually wide spectrum width and can spill over all Fourier components (Fig. 1).

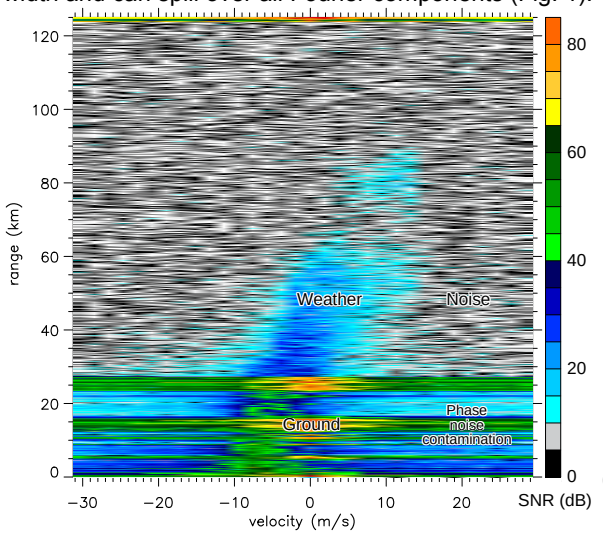

FIG. 1. Power spectrum vs. range of echo intensity (in dB units above noise) computed over 32 pulses collected while scanning over 1° in azimuth. Though the peak contribution from ground targets is centered around zero velocity, ground target echoes can extend to other velocities and exceed weather echoes if they are strong as is the case around 25 km range.

Traditional ground echo identification and filtering try to eliminate (abnormally high) contributions to the echo coming from zero velocity. But in the example shown in Fig. 1, notching velocities near zero would both miss important ground returns and eat much of the weather echoes. Such an approach would hence bias the resulting reflectivity and velocity. And feeding such data to algorithms that do not tolerate biased data or such as those based on data assimilation (e.g., Zawadzki et al. 2009) will lead to the breakdown of those algorithms.

* *Corresponding author address:* Frédéric Fabry, McGill University, Atmospheric and Oceanic Sciences, Montreal, H3A2K6 Canada; e-mail: frederic.fabry@mcgill.ca.

We therefore felt the necessity to revisit the issue of identifying, correcting, and/or censoring echoes that are contaminated by ground targets.

2. AT FIRST TRYING TO BE CLEVER AND FAILING

We initially attempted to take advantage of the predictability of the ground target signature on the raw complex time series of echo returns. Indeed, as you scan over a point ground target, its contribution should follow in power the weighting function of the radar antenna and should be constant in phase (Fig. 2). One should therefore be a lot more selective identifying and suppressing ground targets than simply eliminating all returns with a low velocity. We hence tried to identify Gaussian-shaped elements of constant phase in the raw time series and to eliminate them.

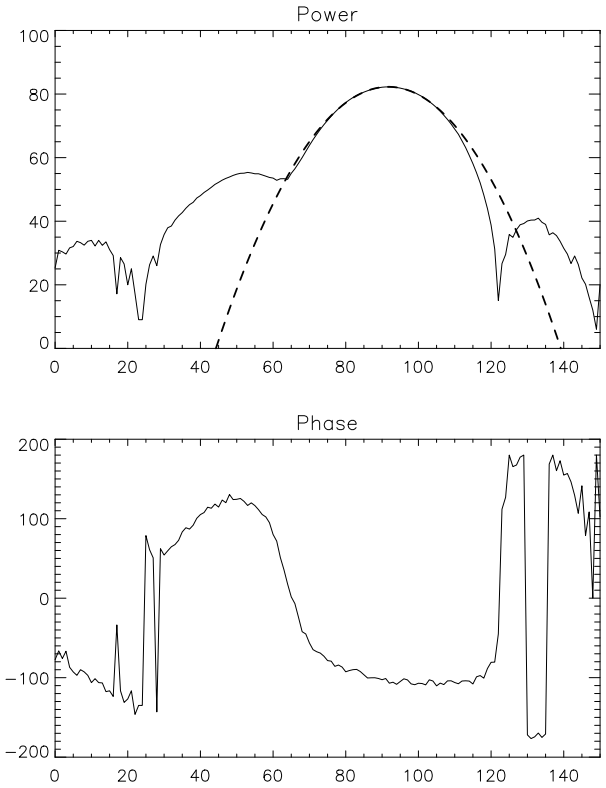

FIG. 2. Time series of power (top, in relative dB units) and phase (bottom, in deg.) of the returns at one range as the radar scans over a reflective ground target over 150 pulses (about 5° in azimuth). The dashed line represents the expected Gaussian beam shape of the radar antenna.

What we did not fully appreciate is the difficulty of properly identifying the Gaussian-shaped elements that belonged to fixed targets but more importantly the fact that the shape of ground echo returns on the time series did not always correspond to a perfect bell curve. For example, when the radar scans at 1° elevation or more, the ground echo that contaminates the returns does not come from the nicely shaped main lobe but from complex sidelobes that do not always resemble the expected Gaussian curve (Fig. 3). A proper removal of these echoes would then require the use of complicated elevation-dependent beam patterns. And even if that were to be done, we did not completely prevent the elimination of weather echoes moving at near-zero velocities. That approach was hence abandoned.

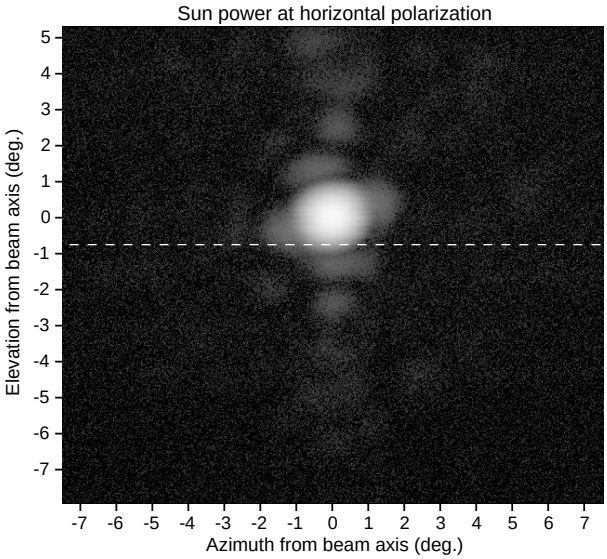

FIG. 3. Our radar antenna beam pattern as a function of elevation and azimuth from axis determined by observing the sun. Brighter regions correspond to stronger antenna gain. The nicely shaped main lobe and the complex sidelobes can be observed easily. The dashed line illustrates the location of ground targets in flat terrain if the radar scans at 0.8° elevation; those targets will be observed both via the bottom side of the main lobe as well as the first bottom-left sidelobe (note the secondary maximum in power near pulse #50 in Fig. 2).

3. MOISSEEV+CHANDRASEKAR TO THE RESCUE

Given this situation, a more general approach was then called for. We decided to explore the information available from dual-polarization returns. We were inspired by the work of Moisseev and Chandrasekar (2009) that used the standard deviation of the spectrum decomposition of Z_{DR} and of φ_{DP} to identify ground targets. The technique is based on the idea that in weather echoes, Z_{DR} and φ_{DP} tend to be consistent from one range gate to the next because of the consistent nature of the target (small targets of near-spheroidal shape), and so should their spectral decomposition $Z_{DR}(k)$ and $\varphi_{DP}(k)$ as a function of the wavenumber k. On the other hand, ground targets are large and complex, and their Z_{DR} and φ_{DP} change from one target to the next. Note that all these ideas should work as well using the raw parameters and their spectral decomposition; the advantage of using their spectral decomposition is that we could isolate on the same bin the contribution coming from ground targets from the one coming from weather.

But to achieve their feat, Moisseev and Chandrasekar (2009), from now on referred to as MC09, went through considerable efforts to use clean spectral estimates (smoothing of spectra over five range bins, spectral windowing using 128 samples, limited sidelobes and phase noise of the CSU-CHILL radar, etc). Could their technique or a variation it work with our noisy data collected at fast operational radar scanning velocity?

Figure 4 shows the spectral decomposition of some of the dual polarization data collected over the same 1° scan seen in Fig. 1. Even on our data, weather targets have $Z_{DR}(k)$ and $\varphi_{DP}(k)$ that are very consistent in both range and k. Ground targets have more varied Z_{DR} and φ_{DP} in range, but that tend to be moderately consistent in k. Finally, noise is… noisy in $Z_{DR}(k)$ and $\varphi_{DP}(k)$. So this first inspection suggests that a reliable spectral-based target identification system is possible.

4. OUR MODIFICATIONS TO MC09

Physically, there is no reason why ground targets should be fluctuating in $Z_{DR}(k)$ and not in $\varphi_{DP}(k)$ or vice versa. Similarly, there is no reason why $Z_{DR}(k)$ and $\varphi_{DP}(k)$ should not be smooth in precipitation targets. As a result, we chose to combine the two standard deviation calculations into one by looking instead at the standard deviation of the complex ratio of the H & V Fourier terms. Given the Fourier terms $H(k)$ and $V(k)$ computed from the raw time series at horizontal and vertical polarization respectively, one can compute $DP(k)$ such that:

$$DP(k) = H(k)/V(k) = 10^{Z_{DR}(k)/20} \exp\left(j\varphi_{DP}(k)\right), \quad (1)$$

where j is the square root of −1. The normalized standard deviation of $DP(k)$,

$$NSD\left[DP(k)\right] = \sqrt{\frac{\sum_{i=-m/2}^{m/2} \left\| DP(k,r+i) - \overline{DP(k,r)} \right\|^2}{(m+1)\left\| \overline{DP(k,r)} \right\|^2}}, \quad (2)$$

was computed over five points only (m=4) and not on a 3x3 area like in MC09. This change was done on the basis that $Z_{DR}(k)$ and $\varphi_{DP}(k)$ did not vary significantly in k for ground targets while it did in r; hence, computing the standard deviation only in range increased the contrast between ground and weather targets. Even though five points is not much, the standard deviation shows dramatically different results for precipitation than for ground targets or noise (bottom right of Fig. 4).

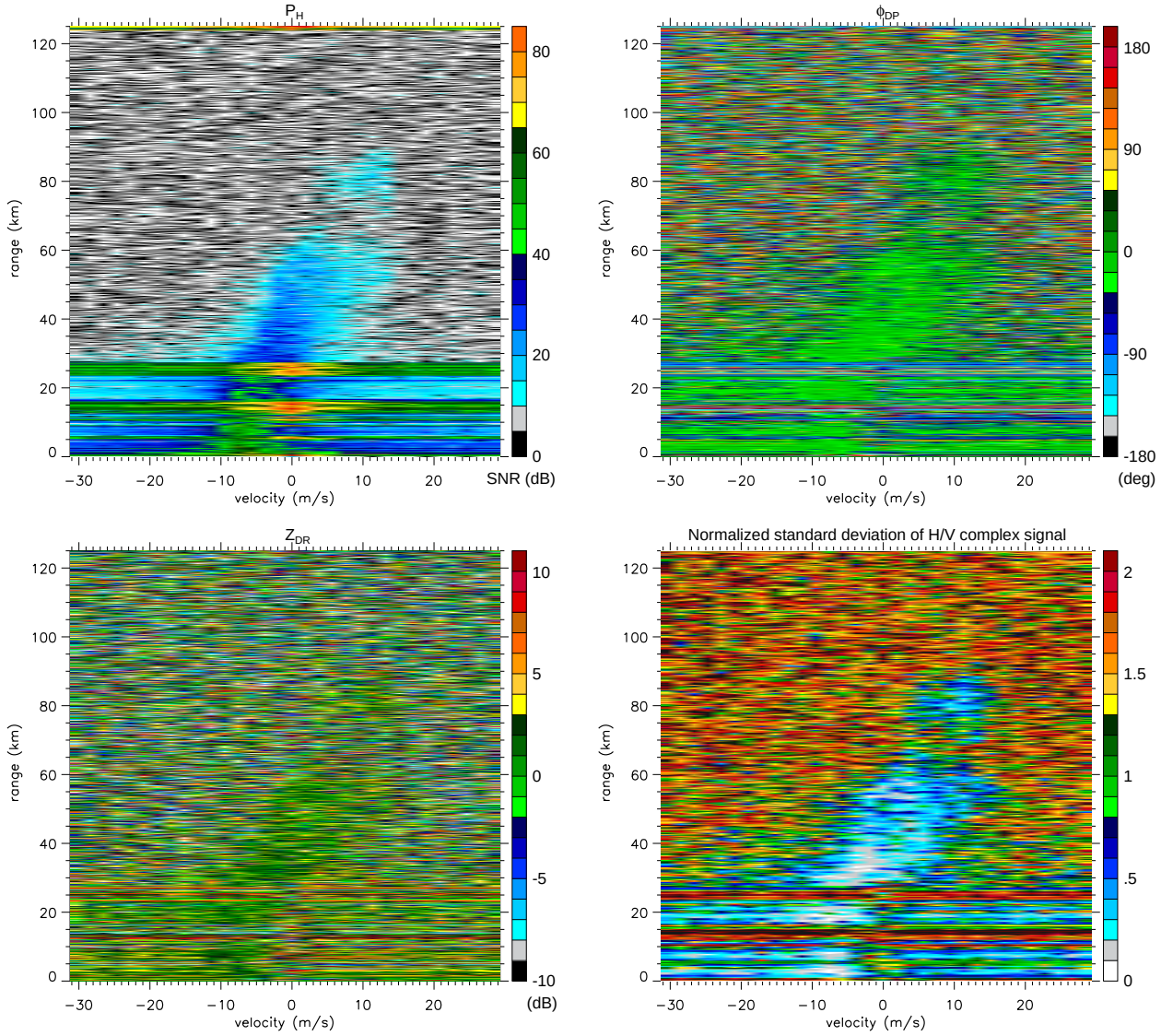

FIG. 4. Power spectrum vs. range of echo intensity (top left), differential phase (top right), and differential reflectivity (bottom left) computed over 32 pulses collected while scanning over 1° in azimuth. On the bottom right is shown the norm of the standard deviation of the ratio of the raw complex time series at H and V polarization which combines the effect of the fluctuations in both Z_{DR} and φ_{DP}.

With different parameters to choose from, we also modified the fuzzy logic approach to combine the information compared with MC09. Figure 5 shows the distribution of *NSD*[*DP*(*k*)] for precipitation, ground targets, and noise. As expected, its value is small in precipitation because of the high coherence in $Z_{DR}(k)$ and in $\varphi_{DP}(k)$, and much larger from ground targets and noise. The use of *NSD*[*DP*(*k*)] for discriminating precipitation and unwanted echoes is hence indicated. While noise and ground targets have similar values in *NSD*[*DP*(*k*)], they will have different SNR and can be easily distinguished.

We hence devise new formulas to assign a score for each spectrum component describing the likelihood that they are fitting the characteristics of precipitation (S_{pre}), ground targets (S_{gnd}), or noise (S_{noi}). We used the following:

$$S_{pre} = .1S_{ZDRpre} + .3S_{SNR} + .6S_{NSDpre}$$

$$S_{gnd}(k=0) = .3\left(.3S_{SNR} + .7S_{NSDgnd}\right) + .7S_{SNR}S_{NSDgnd}$$

$$S_{gnd}(k\neq 0) = .7\left[.3\left(.3S_{SNR} + .7S_{NSDgnd}\right) + .7S_{SNR}S_{NSDgnd}\right] + .3S_{gnd}(k=0)$$

$$S_{noi} = .3\left[.3(1-S_{SNR}) + .7S_{NSDgnd}\right] + .7(1-S_{SNR})S_{NSDgnd}$$

where:

$$S_{ZDRpre} = 0 \text{ if } Z_{DR} > 7\,\text{dB or } Z_{DR} < -5\,\text{dB}$$
$$= 1 \text{ if } -3\,\text{dB} < Z_{DR} < 5\,\text{dB}$$
$$= .5(Z_{DR}+5) \text{ if } -5\,\text{dB} \le Z_{DR} \le -3\,\text{dB}$$
$$= 1 - .5(Z_{DR}-5) \text{ if } 5\,\text{dB} \le Z_{DR} \le 7\,\text{dB}$$

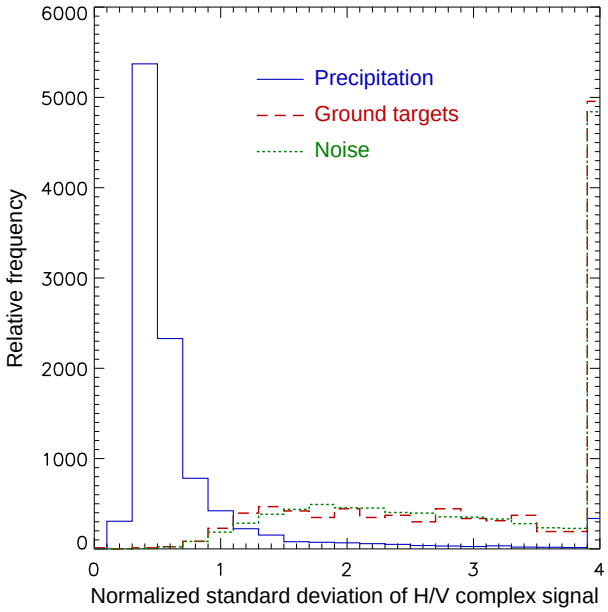

FIG. 5. Histogram of occurrence of NSD[DP(k)] for precipitation (SNR > 15 dB, solid blue line), ground targets (SNR > 15 dB, dashed red line), and noise (dotted green line). The last column represents the occurrence of values larger than 4.

$$
\begin{aligned}
S_{SNR} &= 0 \text{ if } SNR < 0\,\text{dB} \\
&= 1 \text{ if } SNR > 10\,\text{dB} \\
&= .1SNR \text{ if } 0\,\text{dB} \le SNR \le 10\,\text{dB} \\
S_{NSDpre} &= 1 \text{ if } NSD < .7 \\
&= .1 \text{ if } NSD > 2 \\
&= .5 + (1.2 - NSD) \text{ if } .7 \le NSD \le 1.2 \\
&= .1 + .5(2 - NSD) \text{ if } 1.2 \le NSD \le 2 \\
S_{NSDgnd} &= 0 \text{ if } NSD < .5 \\
&= 1 \text{ if } NSD > 1.25 \\
&= 4/3(NSD - .5) \text{ if } .5 \le NSD \le 1.25.
\end{aligned}
\qquad (3)
$$

Got it? ☺

Let us go over the formulas. For precipitation, we give a light weight (10%) for a proper Z_{DR} value (between -3 and +5 dB), ensure that the SNR is strong enough (30% weight), but primarily use the normalized standard deviation of the H/V complex signal (60%). The formulas for the individual score roughly mimic the likelihood of occurrence histograms such as the one shown in Fig. 5. For the ground and noise score, we use the SNR and a score based on *NSD*[*DP*(*k*)] only. The formulas appear much more complicated because of the use of two twists: 1) We use the combination between an additive score (e.g., $.3S_{SNR}+.7S_{NSDgnd}$) that tends to overestimate the fitness into a category and a multiplicative score (e.g., $S_{SNR}S_{NSDgnd}$) that is generally too restrictive. This was important when trying to distinguish ground targets from noise since the only characteristic that differentiated the two was the SNR. 2) For the ground target characterization, we have a different score for the zero velocity and other velocities; at zero velocity, we use the intrinsic properties of the Fourier term to derive a score; at non-zero velocity, we combine the intrinsic properties of the Fourier term with the score at velocity=0 on the grounds that if no ground echo is observed at zero velocity, we are unlikely to see it at other velocities and vice versa. Most of the weights for each term were chosen by trial and error.

A final difference with MC09 is how we determined the different target categories. We chose to have not only the three basic categories (clear precipitation, clearly ground targets, clearly noise) but also "not sure" categories (either precipitation or ground, either precipitation or noise, either ground or noise, undetermined). Answers were deemed "clear" if the top score reached at least 0.5 and exceeded the second score by at least 0.15. When no score reached 0.5 or if all three scores were within 0.15, the "undetermined" category was selected.

5. ID RESULTS AND WHAT NEXT

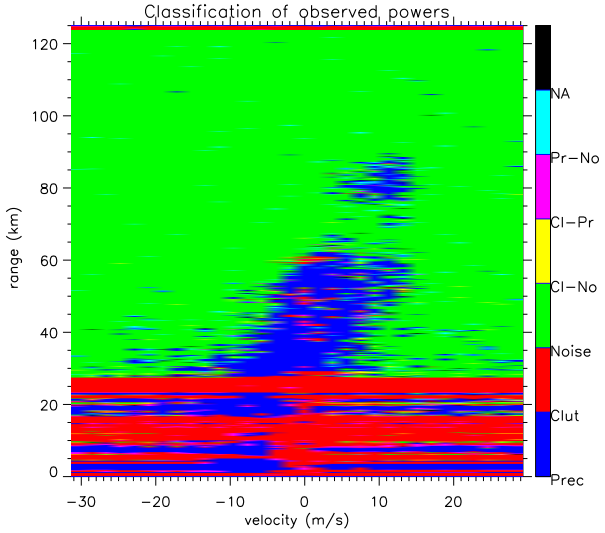

FIG. 6. Classification of targets for the data presented in Figs. 1 and 4.

Figure 6 shows the results of the target ID at the spectrum level. The system was able to detect the echoes contaminated by ground targets not only at zero velocity but also elsewhere. A few precipitation pixels were mistakenly identified as ground targets (e.g., around 55 km near +8 m/s); this occurs when, because of destructive interference, weather echoes at H and V have an unexpected phase difference, resulting in high standard deviations of the H/V ratio as seen by the weak the long tail in the histograms for precipitation in Fig. 5.

If one considers the classification of spectrum data, one can identify "good" targets (precipitation, noise, and either one or the other), and "contaminated" targets (the others). At a given range, one may have either all "good" targets, or all "contaminated" targets, or a mixture. When all targets are "good", the data can be used as is. When all targets are "contaminated", one

might as well have “no data” (different from “no echo”!). For partially contaminated ranges, one can try to fit a Gaussian-shaped spectrum through the “good” data points and fill the “bad” data with the values obtained from the fit. The fraction of the power at a given range obtained through this interpolation process can then be used as a quality index: if less than, say, 20% of the power has been inferred from the interpolation, the information coming from that range bin is likely to still be of high quality; as that fraction increases towards 100%, data quality becomes increasingly poor. This fraction is an important number to keep, as some radar products may be a lot more tolerant than others to errors caused by a bad data correction process. It also has the advantage over “quality indices” to have a rigorous definition.

6. ACKNOWLEDGEMENTS

Thanks to Alamelu Kilambi for providing much of the data used in this work, work that was funded by the Natural Sciences and Engineering Research Council (NSERC) of Canada.

7. REFERENCES

Moisseev, D.N., and V. Chandrasekar, 2009: Polarimetric spectral filter for adaptive clutter and noise suppression. *J. Atmos. Oceanic Tech.*, **26**, 215-228.

Zawadzki, I., K. Chung, A. Kilambi, L. Fillion, and F. Fabry, 2009: From Radio Detection and Ranging (RADAR) to Meso-Analysis System (MAS). Preprints, 34th Conf. on Radar Meteorology, Williamsburg, VA, Amer. Meteor. Soc., paper #13A.1.